Madrigal-Madrigal, J.; Barrera Vilar, D.; Sales Maicas, S. (2019). Refractive Index and Temperature Sensing Using Inter-Core Crosstalk in Multicore Fibers. Journal of Lightwave Technology. 37(18):4703-4709. https://doi.org/10.1109/JLT.2019.2917629

Refractive Index and Temperature Sensing Using Inter-Core Crosstalk in Multicore Fibers

Javier Madrigal, David Barrera, and Salvador Sales, Senior *Member, IEEE*

***Abstract*—Multicore optical fibers are of great interest in the optical sensing field. Their core diversity and spatial distribution enable the development of sensing mechanisms that are not possible in single-core fibers. In this paper we study the use of the inter-core crosstalk phenomena for the implementation of a surrounding refractive index (SRI) sensor. The selective inscription of a tilted fiber Bragg grating (TFBG) intentionally increases the inter-core crosstalk between the inscribed cores and makes it sensitive to the SRI. With this technique we simplify the measurement of the SRI and improve the identification and tracking of the excited cladding modes, as compared with the analysis of the transmission spectrum of a TFBG in single-core fibers. The proposed device is also sensitive to temperature. Temperature is obtained from the crosstalk wavelength shift with a measured sensitivity of 9.75pm/ºC. The SRI is obtained from the measurement of the crosstalk optical power. For increasing SRIs the cladding modes gradually fade, reducing the crosstalk optical power. We observed that the higher the tilt, the higher the sensor sensitivity. For a 7º TFBG the SRI sensitivity obtained is -74.2 dB/RIU from 1.31 to 1.39 and -250.8 dB/RIU from 1.39 to 1.44.**

***Index Terms*—Crosstalk, multicore optical fiber, optical fiber sensors, refractive index, temperature, tilted fiber Bragg gratings.**

I. Introduction

THE refractive index (RI) is one of the most important optical parameters of a material medium. Quick and accurate measurement of the RI plays a key role in chemical composition analysis, measuring concentrations, detecting adulterations and monitoring pollution [1]. In the biological, biomedical and disease diagnosis fields, RI measurement is a key element in determining biophysical parameters, studying metabolic activity and cytometry [2]. The use of refractometers that measure the deviation angle of a light beam passing through a material has been studied in the past [1], while optical fiber sensors are now an expanding research field. These sensors offer numerous advantages for RI measurements: they are small and light, chemically inert and immune to electromagnetic interference. These advantages make them ideal for measuring small sample volumes and for embedding in materials or tissues.

Optical fiber sensors also allow real time remote sensing, distributed sensing, multiparameter sensing, and can work in harsh environments or beside electrical sensors without interference. Many papers have been published on biological or chemical fiber sensors [3-5], mostly those based on measuring the surrounding refractive index (SRI) using different grating types in single core fibers. Fiber Bragg gratings (FBGs) in etched fibers [6-9], D-shape fibers [10,11] and side-polished fibers [12,13] have been proposed in the past. As the geometry of these fibers needs to be modified, this increases production costs. Long period gratings (LPGs) have been used in SRI sensors based on the cladding modes excited by the grating [14,15]. Although these sensors are more sensitive, the length of an LPG limits its use for small point-sensing applications. Tilted fiber Bragg gratings (TFBGs), which combine the advantages of FBGs and LPGs, are an interesting alternative to LPG-based sensors. TFBGs excite more cladding modes and can be shorter than LPGs. Several studies have proposed TFBGs for SRI or multiparameter sensing in single core fibers [16-20].

The recent upsurge of multicore fibers (MCFs) opens up new research possibilities in optical fiber sensing fields. The spatial diversity and distribution of the cores can be used to develop new sensors. Selective grating inscription techniques can take full advantage of multiple cores and are particularly attractive for biochemical applications. Devices with a number of different sensing properties in the same fiber can significantly improve biochemical sensors.

In this paper we use the inter-core crosstalk phenomena to implement a SRI sensor. Crosstalk is naturally present in multicore optical fibers. In optical communications, MCFs are normally designed to minimize crosstalk and maximize the distance between cores or engineering the core refractive index profile to create trenches [21,22]. However, increasing the crosstalk can also be of interest for applications in optical communications and sensing [23,24].

We here propose the use of a low-crosstalk telecommunications MCF and intentionally increase the crosstalk by TFBGs inscribed in the fiber cores [25]. Compared with the traditional TFBG transmission spectrum

This work received support from the Spanish Ministry of Economy and Competitiveness under the DIMENSION TEC2017 88029- R Project, and from the *Generalitat Valenciana* by PROMETEO 2017/017 research excellency award and IDI/FEDER/2018 GVA Infraestructura. J. Madrigal thanks to Universitat Politècnica de València scholarship PAID-01-18 and D. Barrera thanks to Spanish MICINN fellowship IJCI-2017-32476.

J. Madrigal and S. Sales are members of the Photonics Research Labs, ITEAM Research Institute, *Universitat Politècnica de València*, Valencia 46022, Spain (e-mail: jamadmad@iteam.upv.es; ssales@dcom.upv.es). D. Barrera are member of Department of Electronics, University of Alcalá, 28805, Alcalá de Henares, Spain (e-mail: david.barrera@uah.es).

analysis of single-core fibers, this approach has several advantages, such as increasing the signal-to-noise ratio of the cladding modes, improving their identification and tracking, and simplifying the detection of the SRI by measuring the crosstalk power [26].

II. SENSOR DESCRIPTION

The proposed sensor was implemented by the selective inscription of three TFBGs in the cores of an MCF. Selective inscription makes it possible to obtain the full benefit of the spatial distribution of the MCF cores. With this technique, different types of gratings can be inscribed in the fiber's outer cores, making it possible to produce different sensing devices in each core for simultaneous quasi-distributed sensing, multiparameter and multi sensitivity sensing. In this work, we opted to inscribe TFBGs, as they excite the cladding modes, which are sensitive to the external medium. For example, the sensor can be immersed in a sample to obtain its refractive index and temperature. The sensing element is composed of three TFBGs inscribed at the same time by the same production parameters. The TFBGs were selectively inscribed in a row that included the central and outer cores, leaving the rest unaltered.

The sensor principle is based on the crosstalk (XT) between the MCF cores. XT is defined as the relative amount of power transferred from the excited core to another core [27]. Fig. 1 depicts the crosstalk between the different cores in the proposed sensor. The TFBG couples the propagating core mode to multiple cladding modes [16]. In an MCF, a TFBG inscribed in a different core can couple these cladding modes to the forward propagating core mode, increasing the XT [25]. When SRI increases, the cladding modes whose effective refractive index is lower than that of the outer medium are no longer guided and fade, reducing the XT optical power. The cladding modes with the highest effective refractive index are located near the TFBG Bragg wavelength. These cladding modes are known as low order cladding modes and are used to obtain the temperature of the sample under test. Although these modes are not sensitive to SRI, their wavelength is sensitive to strain and temperature stimuli [17,20].

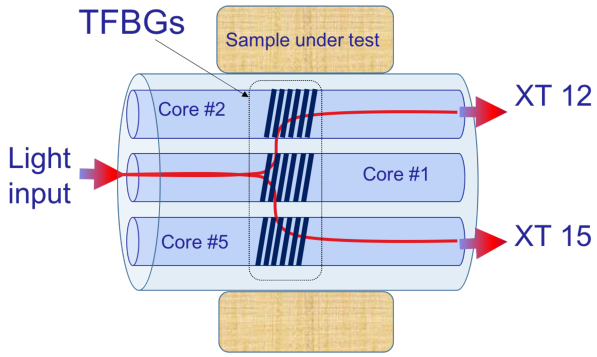

Fig. 1. Sensor scheme showing the cores with TFBGs and the crosstalk. XT12 is the crosstalk when injecting light into core 1 and measuring it in core 2. XT15 is the crosstalk when injecting light into core 1 and measuring it in core 5.

III. GRATING INSCRIPTION

The gratings were inscribed in a commercial 7-core MCF (Fibercore Ltd). The cores are placed in a hexagonal pattern plus a central core. Core spacing is 35 µm and core diameter 5 µm. The numerical aperture is 0.2 and mode field diameter 6.4 µm. The 125 µm cladding diameter is coated with dual acrylate. Prior to inscription, the fiber was hydrogen-loaded in a hydrogen chamber at 50 bar and room temperature for at least 15 days to increase its photosensitivity. The acrylate coating was removed before grating inscription.

Fig. 2 shows the setup used for TFBG inscription by a continuous wave frequency-doubled argon-ion laser emitting at 244nm in a phase mask scanning technique. The phase mask tilt can be adjusted in order to tune the TFBG's properties.

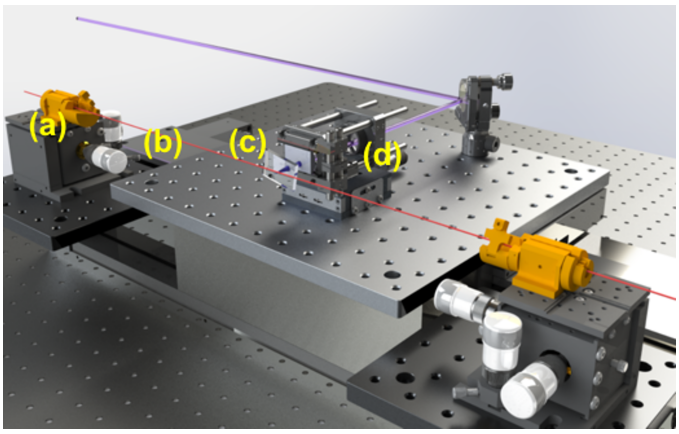

Fig. 2. Inscription setup (a) fiber rotator, (b) multicore fiber, (c) phase mask and (d) set of lenses.

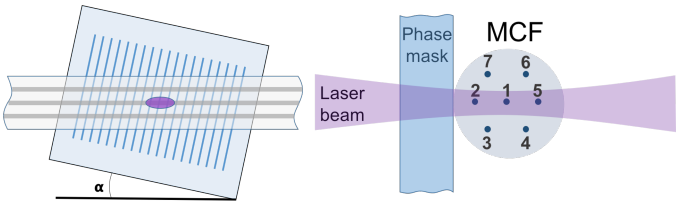

(a) (b)

Fig. 3. (a) Front view of phase mask and fiber. The parameter α indicates the tilt angle. (b) Section view of the aligned fiber and the cores position during the incription.

Selective inscription requires accurate control of the core position and laser beam size, which was adjusted to irradiate one row of cores only, using a set of lenses. The core position was adjusted by a core tracking subsystem. The phase mask is previously removed from the inscription setup. When exposed to UV radiation, a photoluminescence signal is generated and guided by the cores of the fiber and finally photodetected [28,29]. The tracking subsystem can deflect the laser beam in order to maximize photoluminescence. The amount and direction of this deflection indicates the position of each core inside the fiber. To align the cores, the fiber can be rotated until the tracking subsystem indicates that the three cores are

in the same position. We have used this selective alignment technique successfully in previous studies to inscribe TFBGs, FBGs and LPGs in different rows [25,30, 31].

When the cores were correctly aligned, the phase mask was placed in the setup and tilt was adjusted as appropriate. Fig. 3 shows the scheme of the phase mask and the aligned fiber. Two sensors were inscribed in independent fibers with the same TFBG length of 5mm and tilt angles of α=2º and α=7º. The phase mask periods used were 1073.73nm for the 2º TFBG and 1083.60nm for the 7º TFBG. Two fan in/out devices (Optoscribe Ltd) were spliced to both ends of the MCF to connect each MCF core to a single fiber. The fan in/out devices were used to inject the input light into one core at the end of the fiber and XT was measured in another core at the other end. Fig. 4 shows the transmission spectra of the three inscribed cores and the transmission spectrum of a non-aligned core for the 2º and 7º TFBG sensors.

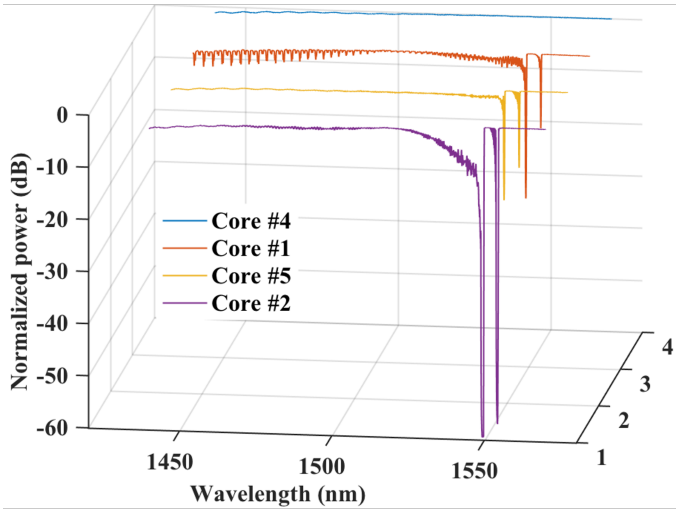

(a)

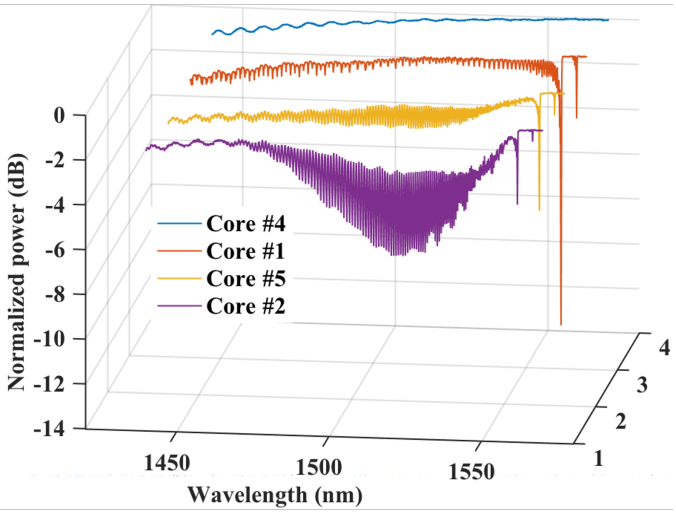

(b)

Fig. 4. Spectrum of the TFBGs inscribed in cores 1, 2 and 5 for both sensors. (a) 2º TFBGs spectra and (b) 7º TFBGs spectra. The rest of the cores have a similar spectrum to core 4.

IV. SENSOR CHARACTERIZATION SETUP AND EXPERIMENTAL RESULTS

The sensors were characterized for temperature and SRI changes. Fig. 5 shows a photograph of the sensor characterization setup. The fiber was fixed between two 3-axis moving platforms to keep it straight, avoid rotation and control its position. The part of the fiber with the TFBGs was placed in the middle of the platforms. A small aluminum cuvette was made to immerse the fiber in different RI dilutions. The cuvette was mounted on a z-axis platform to adjust its height. A Peltier thermoelectric module driven by an electronic controller was used to set the liquid temperature and keep it constant during the measurements. The Peltier module was fixed underneath the cuvette with thermal compound to optimize heat transfer.

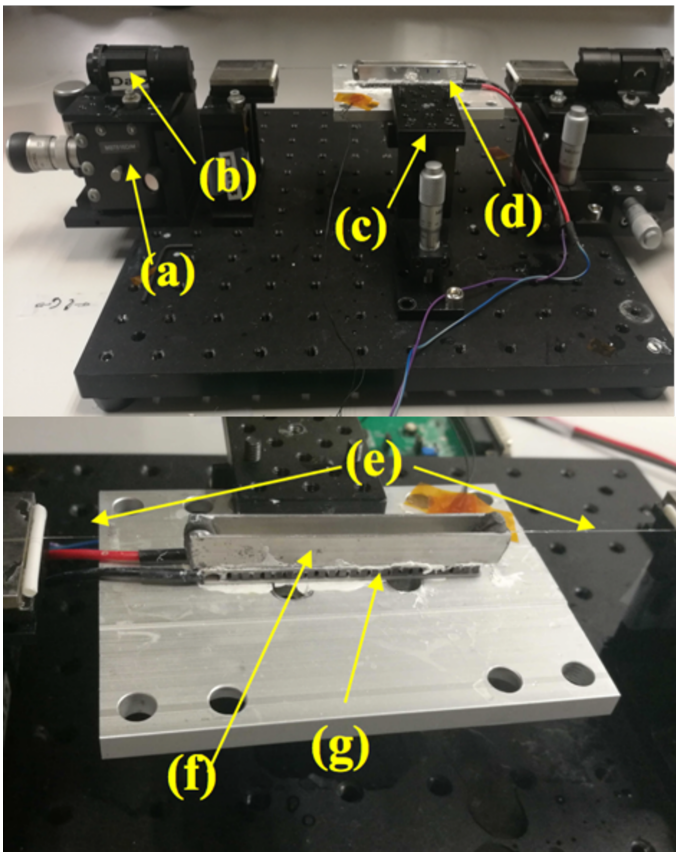

Fig. 5. (Top) View of the sensor characterization setup: complete setup. (a) Translation stage, (b) rotation stage, (c) z-axis stage, and (d) cuvette. (Bottom) Detail of the cuvette: (e) fiber, (f) cuvette, and (g) Peltier module.

XT was then measured using two TS100HP tunable lasers with a Yenista CT400 component analyzer. The light was injected into one core and the XT was measured in another core at the other end. XTAB denotes the crosstalk measured when injecting light into core A and measuring it in core B.

Fig. 6 and Fig. 7 compare the crosstalk spectra when the light is injected into core 5 for the 2º TFBG and the 7º TFBG. Crosstalk measured in a core without TFBG (XT54) is much smaller than the crosstalk between the cores with TFBG, while the crosstalk between the outer cores (XT52) is even higher.

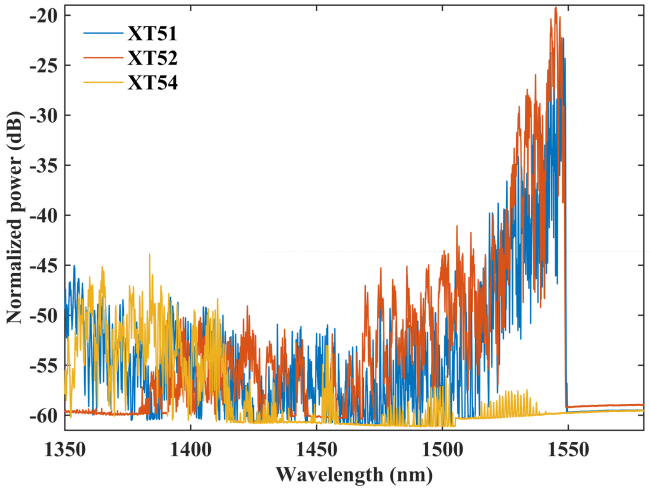

Fig. 6. XT51, XT52 and XT54 spectra for the 2º TFBG. The power was normalized to the input power.

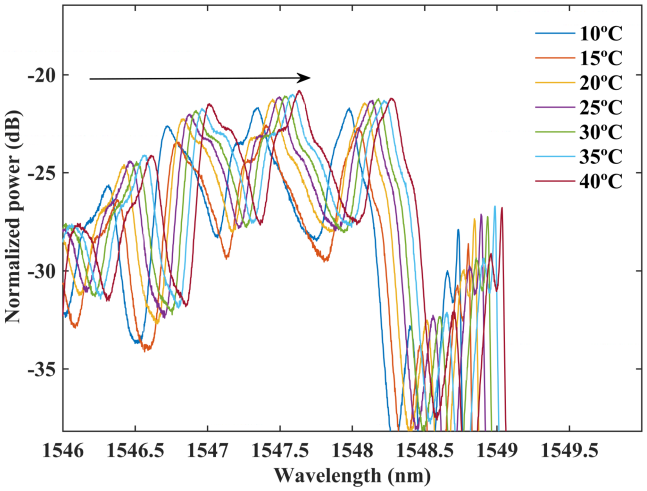

Fig. 8. XT12 spectrum at different temperatures. The arrow indicates the increasing temperature direction.

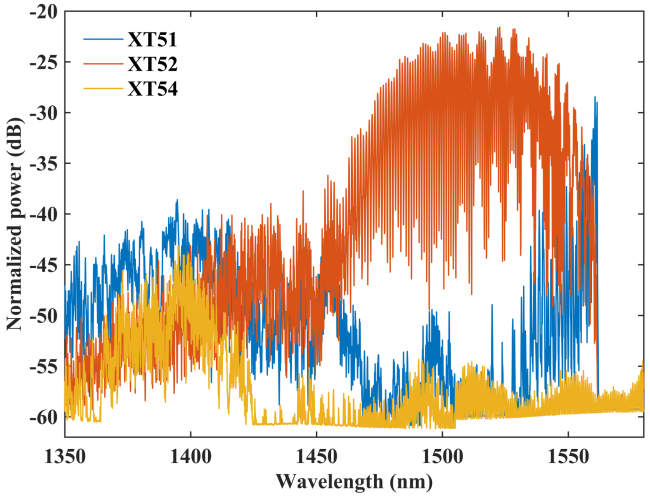

Fig. 7. XT51, XT52 and XT54 spectra for the 7º TFBG. The power was normalized to the input power.

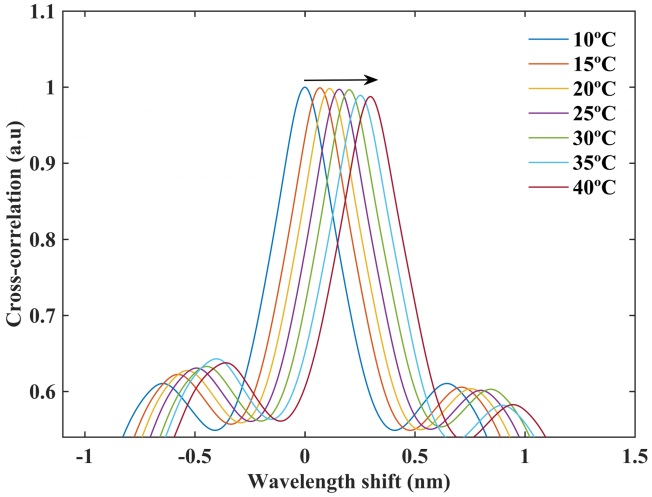

Fig. 9. Calculated cross-correlation of crosstalk XT12 spectrum at different temperatures with XT12 spectrum at 10ºC. The arrow indicates the increasing temperature direction.

To characterize the sensor under temperature changes, the 2º TFBG was immersed in pure water whose temperature was raised from 10º to 40º in 5ºC increments. All the possible XT combinations between cores 1, 2 and 5 were measured at each step. Fig. 8 shows a detail of the XT12 spectrum at the different temperatures.

Taking the XT spectra at 10ºC as reference, we used the peak tracking correlation method [32] from 1546 to 1550 nm to measure the wavelength shift of all the peaks. Fig. 9 shows the cross-correlation between the XT12 spectrum at 10ºC and the XT12 spectrum for higher temperatures.

The wavelength shift for all the crosstalk combinations is detailed in Fig. 10. It can be seen that the XT spectrum undergoes a red wavelength shift when the temperature is raised. This wavelength shift is the same in all the measurements as it is a consequence of the TFBG shift with temperature. Since the fiber is not bent, the temperature sensitivity of all the cores is the same. The XT wavelength temperature sensitivity obtained was 9.75pm/ºC.

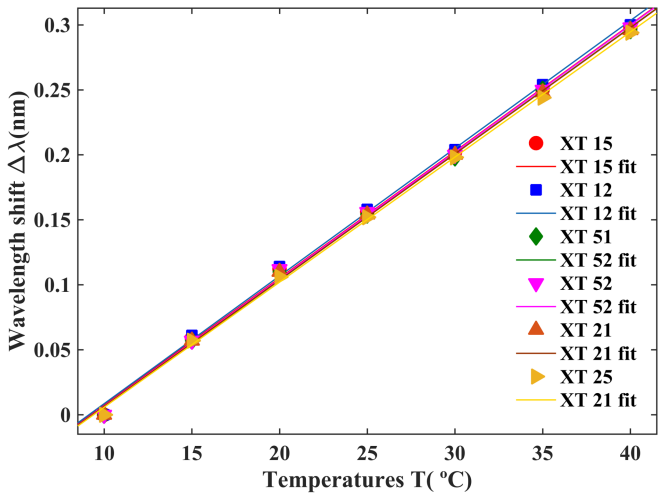

Fig. 10. Wavelength shift vs temperature for all crosstalk combinations. The plotted lines indicate the linear fitting applied to the wavelength shift data.

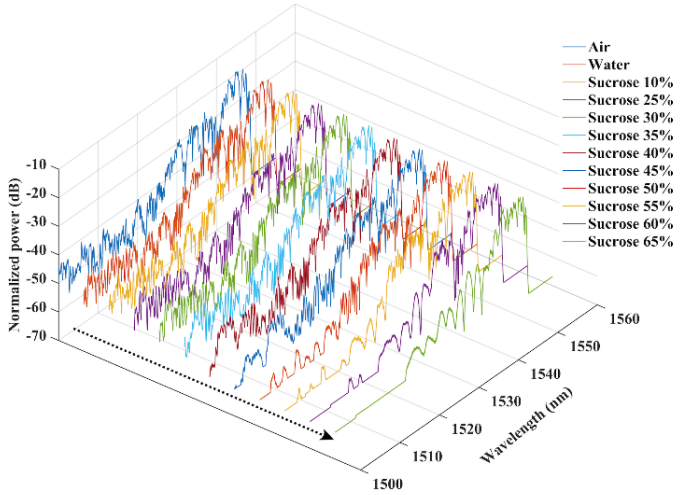

Fig. 11. Spectra for XT52 when the 2º TFBG sensor was immersed in different sucrose dilutions i.e., different SRI. The arrow indicates the increasing SRI direction.

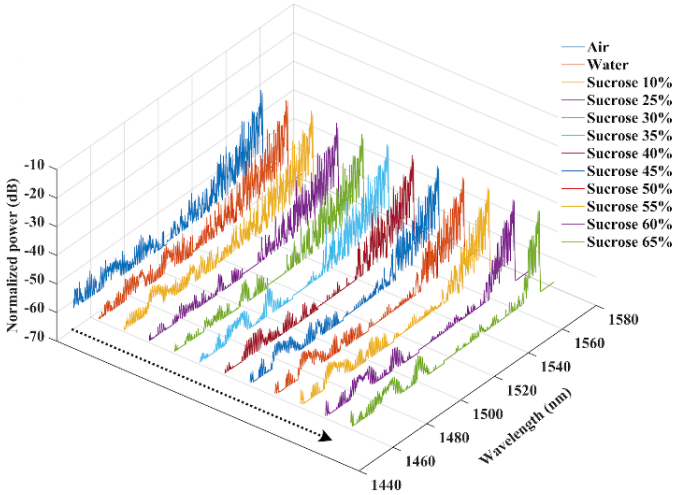

Fig. 13. Spectra for XT15 when the 7º TFBG sensor was immersed in different SRI i.e., different sucrose dilutions. The arrow indicates the increasing SRI direction.

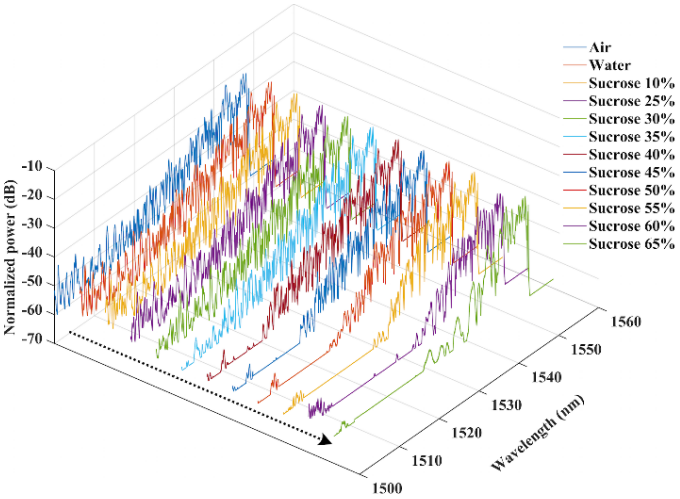

Fig. 12. Spectra for XT12 when the 2º TFBG sensor was immersed in different sucrose dilutions. The arrow indicates the increasing SRI direction.

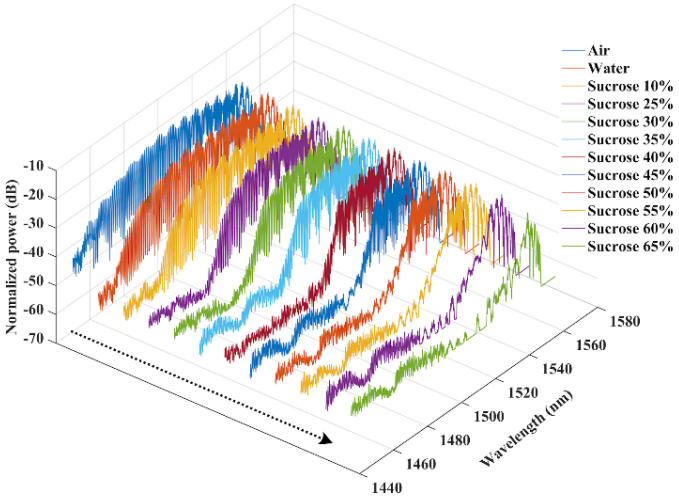

Fig. 14. Spectra for XT25(b) when the 7º TFBG sensor was immersed in different SRI i.e., different sucrose dilutions. The arrow indicates the increasing SRI direction.

For the SRI experiments the sensors were immersed in different dilutions of sucrose and pure water at a constant 25 ºC. At every dilution change the cuvette and fiber were cleaned with pure hot water and then dried to remove any traces of the previous dilution. The concentrations used were 0 wt.%, 10 wt.%, and from 25 wt.% to 65 wt.% in increments of 5 wt.%. The refractive index of the sucrose dilution increased with concentration. The SRI obtained using the sucrose concentrations was in the range from 1.3166 to 1.4370, in agreement with [33]. The XT between cores inscribed with TFBGs was measured for each dilution.

Fig. 11 and Fig. 12 show the XT12 and the XT52 measured in the 2º TFBG sensor immersed in different SRI. The XT spectra were normalized to the input power. XT power faded as SRI increased.

The 7º TFBG sensor was measured following the same procedure as for the 2º TFBG sensor. Fig. 13 and Fig. 14 show the XT15 and the XT25 measured in the 7º TFBG sensor immersed in different SRI. The XT is seen to fade with higher SRI. The 7º TFBG sensor experienced greater XT fading than the 2º TFBG sensor, particularly in the case of XT25 and XT52.

Crosstalk power fading with SRI was studied and total crosstalk power was calculated integrating the spectrum and normalized to the crosstalk power when the SRI is 1. Fig.15 shows crosstalk power fading with SRI for all possible combinations. XT power showed a monotonic decreasing trend with the SRI.

The results obtained indicate that crosstalk power is sensitive to SRI and decreases as SRI increases. For the 2º TFBG all the XT measurements behaved similarly. The mean SRI sensitivity is approximately -9.92 dB/RIU from 1.31 to 1.39 and -49.6 dB/RIU from 1.39 to 1.44. In the 7º TFBG sensor XT25 and X52 decayed significantly more than the rest of XT measurements. The mean sensitivity obtained using X25 and X52 is approximately -74.2 dB/RIU from 1.31 to 1.39 and -250.8 dB/RIU from 1.39 to 1.44.

The use of a higher tilt angle increases the number of cladding modes excited. This effect is more clearly seen in the XT between the two external cores. These additional cladding modes, which have a lower effective refractive index, fade for lower SRIs, so that SRI sensitivity is higher for the 7º TFBG.

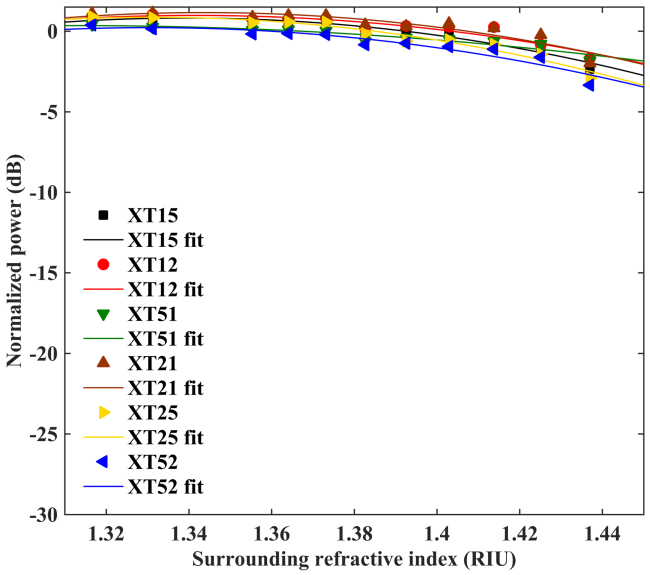

(a)

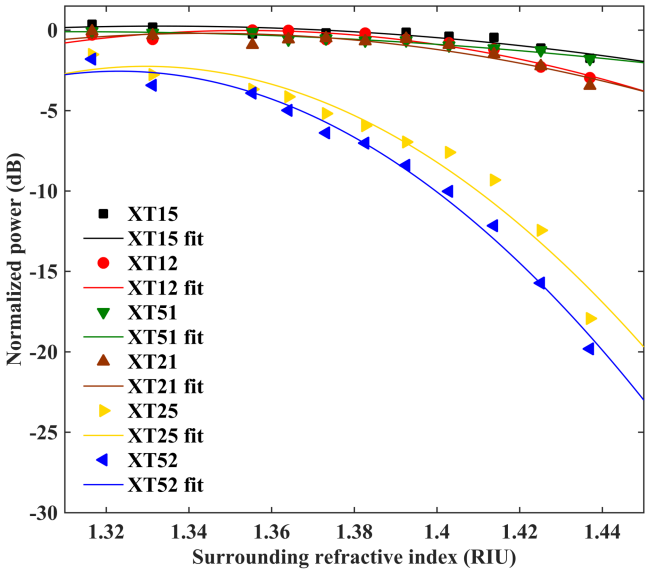

(b)

Fig. 15. XT power fading vs the SRI for both sensors. (a) 2º TFBG sensor and (b) 7ºTFBG sensor. All the possible XT combinations are plotted between the cores with inscribed TFBGs. The plotted curves are the second order polynomial fitting.

V. CONCLUSIONS

The use of multicore optical fibers permits the use of different sensing techniques. In this paper we demonstrate the use of tilted fiber Bragg gratings to increase inter-core crosstalk and make it sensitive to temperature changes and the surrounding refractive index. Compared to the use of standard single-core fibers, this approach improves the signal-to-noise ration of the cladding modes and simplifies SRI measurement by measuring the crosstalk power. We show that the inter-core crosstalk spectrum undergoes a 9.75pm/ºC wavelength shift and that crosstalk power fades when the SRI increases in a monotonic decreasing trend. Comparing the performance of a 2º TFBG and a 7º TFBG, we found that the higher the tilt angle, the higher the power fade and sensitivity. In the 7º TFBG, the crosstalk power fade between the two external cores is -74.2 dB/RIU from 1.31 to 1.39 and -250.8 dB/RIU from 1.39 to 1.44.

REFERENCES

[1] S. Singh, "Refractive Index Measurement and its Applications," *Physica Scripta*, vol. 65, no. 2, pp. 167–180, Jan. 2002.

[2] P. Y. Liu, L. K. Chin, W. Ser, H. F. Chen, C.-M. Hsieh, C.-H. Lee, K.-B. Sung, T. C. Ayi, P. H. Yap, B. Liedberg, K. Wang, T. Bourouina, and Y. Leprince-Wang, "Cell refractive index for cell biology and disease diagnosis: past, present and future," *Lab on a Chip*, vol. 16, no. 4, pp. 634–644, Dec. 2015.

[3] M. Pospíšilová, G. Kuncová, and J. Trögl, "Fiber-Optic Chemical Sensors and Fiber-Optic Bio-Sensors," *Sensors*, vol. 15, no. 10, pp. 25208–25259, Sept. 2015.

[4] X.-D. Wang and O. S. Wolfbeis, "Fiber-Optic Chemical Sensors and Biosensors (2013–2015)," *Analytical Chemistry*, vol. 88, no. 1, pp. 203–227, Mar. 2015.

[5] F. Chiavaioli, F. Baldini, S. Tombelli, C. Trono, and A. Giannetti, "Biosensing with optical fiber gratings," *Nanophotonics*, vol. 6, no. 4, Jan. 2017.

[6] P. Ray, S. K., and B. Srinivasan, "Enhanced sensitivity etched fiber Bragg gratings for precise measurement of refractive index," in *Proc. SPIE 9654International Conference on Optics and Photonics*., Kolkata, India, 2015.

[7] W. Liang, Y. Huang, Y. Xu, R. K. Lee, and A. Yariv, "Highly sensitive fiber Bragg grating refractive index sensors," *Applied Physics Letters*, vol. 86, no. 15, p. 151122, Apr. 2005.

[8] A. Iadicicco, A. Cusano, S. Campopiano, A. Cutolo, and M. Giordano, "Thinned fiber Bragg gratings as refractive index sensors," IEEE Sensors Journal, vol. 5, no. 6, pp. 1288–1295, Dec. 2005.

[9] A. Chryssis, S. Saini, S. Lee, H. Yi, W. Bentley, and M. Dagenais, "Detecting hybridization of DNA by highly sensitive evanescent field etched core fiber Bragg grating sensors," *IEEE Journal of Selected Topics in Quantum Electronics*, vol. 11, no. 4, pp. 864–872, July-Aug. 2005.

[10] K. Zhou, X. Chen, L. Zhang, and I. Bennion, "Implementation of optical chemsensors based on HF-etched fibre Bragg grating structures," *Measurement Science and Technology*, vol. 17, no. 5, pp. 1140–1145, Apr. 2006.

[11] T. L. Lowder, J. D. Gordon, S. M. Schultz, and R. H. Selfridge, "Volatile organic compound sensing using a surface-relief D-shaped fiber Bragg grating and a polydimethylsiloxane layer," *Optics Letters*, vol. 32, no. 17, p. 2523, Sep. 2007.

[12] K. Schroeder, W. Ecke, R. Mueller, R. Willsch, and A. Andreev, "A fibre Bragg grating refractometer," *Measurement Science and Technology*, vol. 12, no. 7, pp. 757–764, Jul. 2001.

[13] Z. Chen, J. Tang, R. Fan, Y. Zhong, J. Zhang, and S. Li, "Side polished fiber Bragg grating sensor for simultaneous measurement of refractive index and temperature," in *Proc*. SPIE 7753 *OFS-21*., Ottawa, Canada, 2011.

[14] S. W. James and R. P. Tatam, "Optical fibre long-period grating sensors: characteristics and application," *Measurement Science and Technology*, vol. 14, no. 5, Mar. 2003.

[15] M. Janczuk-Richter, M. Dominik, E. Roźniecka, M. Koba, P. Mikulic, W. J. Bock, M. Łoś, M. Śmietana, and J. Niedziółka-Jönsson, "Long-period fiber grating sensor for detection of viruses," Sensors and Actuators B: Chemical, vol. 250, pp. 32–38, Oct. 2017.

[16] J. Albert, L.-Y. Shao, and C. Caucheteur, "Tilted fiber Bragg grating sensors," *Laser & Photonics Reviews*, vol. 7, no. 1, pp. 83–108, Feb. 2012.

[17] T. Guo, F. Liu, B.-O. Guan, and J. Albert, "Tilted fiber grating mechanical and biochemical sensors," *Optics & Laser Technology*, vol. 78, pp. 19–33, Apr. 2016.
[18] Y.-P. Miao, B. Liu, and Q.-D. Zhao, "Refractive index sensor based on measuring the transmission power of tilted fiber Bragg grating," *Optical Fiber Technology*, vol. 15, no. 3, pp. 233–236, June 2009.
[19] G. Laffont and P. Ferdinand, "Tilted short-period fibre-Bragg-grating-induced coupling to cladding modes for accurate refractometry," *Measurement Science and Technology*, vol. 12, no. 7, pp. 765–770, Aug. 2001.
[20] C. Caucheteur, K. Chah, F. Lhomme, M. Blondel, and P. Megret, "Simultaneous bend and temperature sensor using tilted FBG,"in Proc. *SPIE* 5855 17th International Conference on Optical Fibre Sensors, Bruges, Belgium, 2005.
[21] K. Saitoh, M. Koshiba, K. Takenaga, and S. Matsuo, "Crosstalk and Core Density in Uncoupled Multicore Fibers," *IEEE Photonics Technology Letters*, vol. 24, no. 21, pp. 1898–1901, 2012.
[22] T. Hayashi, T. Taru, O. Shimakawa, T. Sasaki, and E. Sasaoka, "Characterization of Crosstalk in Ultra-Low-Crosstalk Multi-Core Fiber," *Journal of Lightwave Technology*, vol. 30, no. 4, pp. 583–589, 2012.
[23] J. Villatoro, E. Antonio-Lopez, A. Schülzgen, and R. Amezcua-Correa, "Miniature multicore optical fiber vibration sensor," *Optics Letters*, vol. 42, no. 10, p. 2022, 2017.
[24] A. M. T. Almeida, R. N. Nogueira, and M. Facão, "Analysis of power transfer on multicore fibers with long-period gratings," *Optics Letters*, vol. 40, no. 2, p. 292, 2015.
[25] D. Barrera, J. Madrigal, and S. Sales, "Tilted fiber Bragg gratings in multicore optical fibers for optical sensing," *Optics Letters*, vol. 42, no. 7, p. 1460, Apr. 2017.
[26] J. Madrigal, D. Barrera, and S. Sales, "Refractive index and temperature sensor based on TFBGs in multicore fiber," *26th International Conference on Optical Fiber Sensors*, Lausanne, Switzerland, 2018, paper ThE11.
[27] L. Szostkiewicz, M. Napierala, A. Ziolowicz, A. Pytel, T. Tenderenda, and T. Nasilowski, "Cross talk analysis in multicore optical fibers by supermode theory," *Optics Letters*, vol. 41, no. 16, p. 3759, Aug. 2016.
[28] M. Gallagher and U. Österberg, "Time resolved 3.10 eV luminescence in germanium-doped silica glass," *Applied Physics Letters*, vol. 63, no. 22, pp. 2987–2989, Sep. 1993.
[29] T. Komukai and M. Nakazawa, "Fabrication of high-quality long-fiber Bragg grating by monitoring 3.1-eV radiation (400 nm) from GeO defects," *IEEE Photon. Technol. Lett*., vol. 8, no. 11, pp. 1495–1497, Nov. 1996.
[30] I. Gasulla, D. Barrera, J. Hervás, and S. Sales, "Spatial Division Multiplexed Microwave Signal processing by selective grating inscription in homogeneous multicore fibers," *Scientific Reports*, vol. 7, no. 1, Jan. 2017.
[31] D. Barrera, J. Madrigal, and S. Sales, "Long Period Gratings in Multicore Optical Fibers for Directional Curvature Sensor Implementation," *Journal of Lightwave Technology*, vol. 36, no. 4, pp. 1063–1068, Feb. 2018.
[32] D. Tosi, "Review and Analysis of Peak Tracking Techniques for Fiber Bragg Grating Sensors," *Sensors*, vol. 17, no. 10, p. 2368, Sep. 2017.
[33] J. E. Saunders, C. Sanders, H. Chen, and H.-P. Loock, "Refractive indices of common solvents and solutions at 1550 nm," *Applied Optics*, vol. 55, no. 4, p. 947, Feb. 2016.